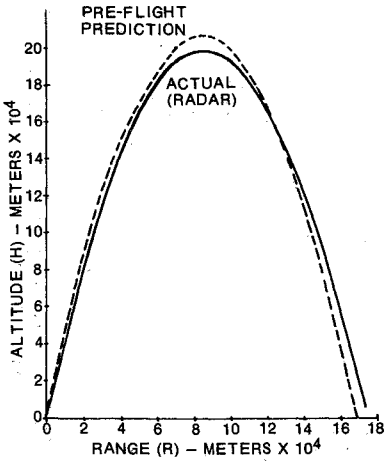


Fig. 5 Flight test vehicle trajectory.

3) Burnout roll rate was 3.4 rev/sec; the fins were set to produce a theoretical 2.5 rps. However, fin conduit facing interference effects were unaccounted for.

4) Burnout velocity was 1737 m/sec at an altitude of 48 km; predicted values were 1772 m/sec and 46 km. Performance was near predicted (Fig. 5).

5) Longitudinal acceleration averaged about 11.5$g$ during boost phase, dropped to about 1$g$ at boost phase burnout, then rose to a sustain phase maximum of about 6.3$g$ at $t+38$ sec.

6) No significant temperature rise occurred anywhere on the motor during burn. Payload temperature was of the order of magnitude expected (Fig. 6).

7) Vibration input to the payload, once the vehicle was out of the tower, varied from about 1.2$g$ to about 4$g$, peak to peak, at about 1 kHz in the lateral planes and from about 1.5$g$ to 3$g$, 1 kHz in the thrust direction.

8) The vehicle exited the tower at $t+0.96$ sec with a velocity of 84.5 m/sec.

9) The two lateral accelerometers in the tail show a peak to peak vibration of 10$g$–12$g$ at moderate frequencies. The apparent correlation between the amplitude-time characteristic of this vibration and the dynamic pressure vs time curve suggests that the observed vibration is influenced by, perhaps dominated by, aerodynamics rather than the motor and is most likely due to interactive flow phenomena between the conduits and the fins which were not aligned with each other.

10) The recovery of the vehicle failed because the fins were not jettisoned.

The main parachute, its bag, the flotation bag and its bag, and portions of the drogue chute bag were recovered. Entangled in the mass of nylon and webbing were a number of fragments from the recovery system itself and from the payload, indicating that the vehicle payload section of the vehicle disintegrated at impact.

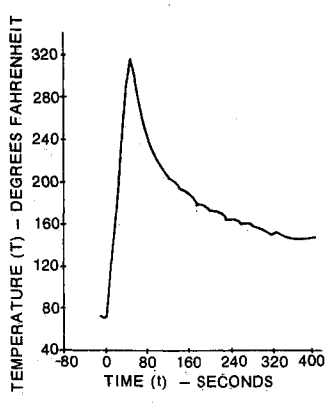


Fig. 6 Forward skirt door temperature.

**Summary**

A successful program for the demonstration of a new propulsion system with the stated new technology features and the integration of this motor into a flight vehicle was accomplished.

**References**

[1] Jenkins, R. B. and Taylor, J. P., "Astrobee D—An Advanced Technology Boost/Sustain Meteorological Rocket Vehicle," AIAA Paper 70-1387, Williamsburg, Va., 1970.

[2] Coanda, H., "Analysis of Thrust Due to the Coanda Phenomenon," Contract Rept. AF 61(052)-382, Oct. 29, 1960, U.S. Air Force, Washington, D.C.

# Blowing Simulation of Asymmetric Transition Effects on Slender Ablating Vehicles

LARS E. ERICSSON*
*Lockheed Missiles & Space Company, Inc., Sunnyvale, Calif.*

THE effects of aft body asymmetric transition on slender vehicle aerodynamics as measured by Martellucci and Neff,[1] using blowing to simulate ablative mass addition, seem to be in sharp contrast to what has been presented in Ref. 2 (see Fig. 1). The negative aerodynamic loading induced by asymmetric transition should have the highest slope at $\alpha = 0$ and not at some intermediate value like $\alpha = 0.5°$.

In order to understand the peculiar behavior of the transition-induced characteristics in Fig. 1, the author consulted the data source.[3] As sketched in the insets in Fig. 2, there are two important $\alpha$-parameters in a test simulating asymmetric transition effects on an ablating model using blowing. The blowing area was shaped to conform to the free transition front measured on the nonblowing solid model (with smooth surface) at a certain angle of attack $\alpha = \alpha_{AT}$. The aerodynamic loads for various blowing rates were then measured as a function of $\alpha$ for three blowing geometries, i.e., those with blowing fronts corresponding to the transition lines for $\alpha_{AT} = 0°$, 1°, and 2°. The freestream unit Reynolds number was kept constant at the value used when defining the transition front geometry on the solid model.

Even when the transition front is far upstream of the base, thereby minimizing the sting interference which (otherwise) can be large for models with boundary-layer mass addition,[4] one faces several problems when attempting this type of simulation of asymmetric transition effects, as is discussed by Martellucci and Neff.[1] Using an impervious forward section for the laminar flow region may give the turbulent blowing rate increment a larger effect than it has in presence of forebody blowing (at laminar levels). At low blowing rates the breathing and tripping effects of the porous surface itself also have to be considered.[5–8]

In spite of these simulation difficulties, one can postulate that at some angle of attack close to $\alpha = \alpha_{AT}$ the free† transition effect is indeed simulated. With this in mind the author went

Presented as Appendix of AIAA Paper 73-126 at the AIAA 11th Aerospace Sciences Meeting, Washington, D.C., January 10–12, 1973; submitted April 13, 1973; revision received September 13, 1973.

Index categories: Boundary Layer Stability and Transition; Jets, Wakes, and Viscid-Inviscid Flow Interactions; Entry Vehicle Dynamics and Control.

* Consulting Engineer. Associate Fellow AIAA.

† "Free" means with transition free to move with $\alpha$, as is the case on the ablating flight vehicle.

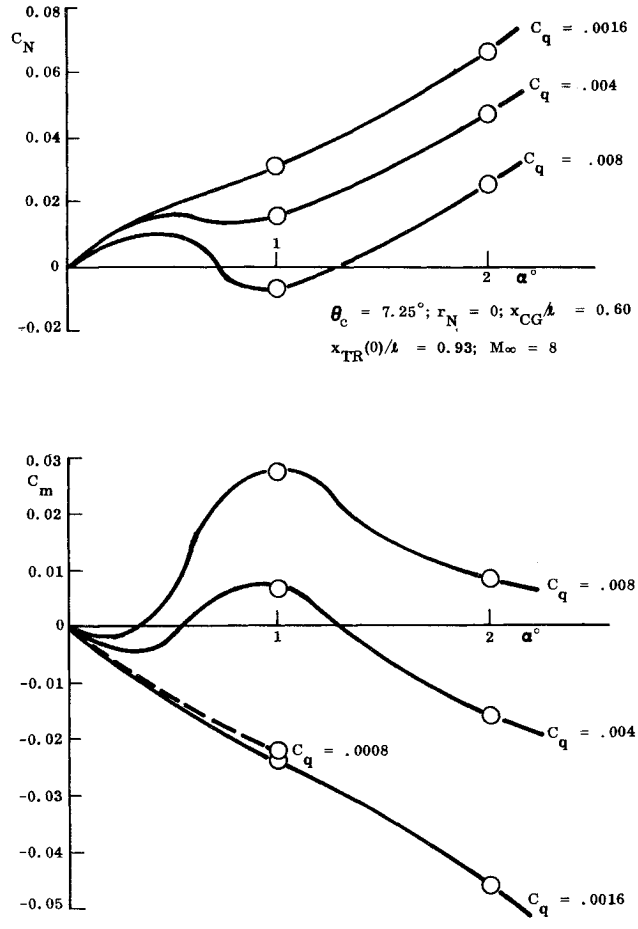


Fig. 1 Effect of asymmetric blowing on $C_N(\alpha)$ and $C_m(\alpha)$-characteristics.

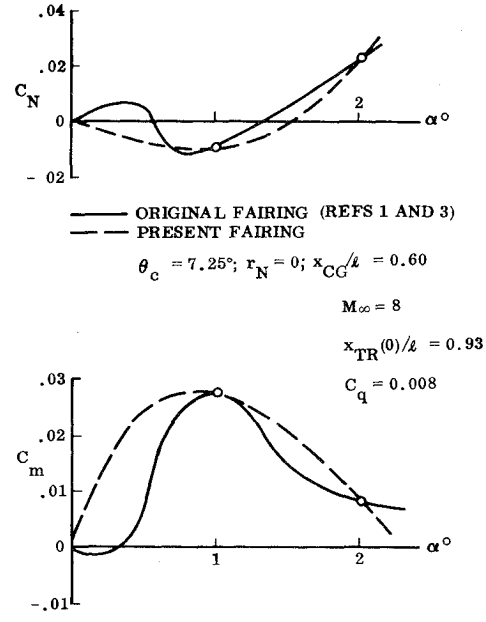


Fig. 3 Effect of asymmetric transition-blowing on slender cone aerodynamic characteristics.

to the original data[3] and carpet-plotted[9,10] them as functions of $\alpha$ and $\alpha_{AT}$. A sample result is shown in Fig. 2 ($C_m$ for one blowing rate, $C_q = 0.008$, and one mean transition location) $X_{TR}(0)/l = 0.93$. Following the data for the ($\alpha_{AT} = 2°$)-configuration, one can visualize what happens from the inset-sketches. The "breakaway" for $\alpha < \alpha_{AT}$ is most likely caused by the aft movement of transition and associated region of increased self-induced pressures.[2] At $\alpha > \alpha_{AT}$ natural transition occurs upstream of the blowing area. The associated forward movement of transition and the self-induced pressure effect in the nonblowing upstream region generates loads that are negligibly small compared to the (unchanged) effect of the downstream blowing (into a turbulent boundary layer).

Assuming that free transition is simulated at $\alpha = \alpha_{AT}$, the combined effects of $\alpha$ *and* $\alpha_{AT}$ are measured only at $\alpha = \alpha_{AT}$. The dashed line drawn through these data points in Fig. 2 represents the effect of free transition line movement, with the mass addition downstream of transition staying at a constant level, $C_q = 0.008$. The normal force data can be reduced in the same manner, and the final results are as shown in Fig. 3. The fairing obtained through the carpet-plotting procedure is quite different from the one suggested by the original investigators.[1,3] If experimental data for $\alpha_{AT} = 0.5°$ had been obtained, the two fairings would probably be less different. However, there is always a limit to how many data points one can afford to obtain in a test. In order to make every data point count, carpet-plotting of hypothetical data should be undertaken in the planning phase of a test.[9]

In order to answer one argument that may arise, i.e., "Why should one believe one fairing more than the other," the following observations are presented. In the carpet-plot (Fig. 2) there are only two actual experimental data points for the combined effect of $\alpha$ and $\alpha_{AT}$. Those are at $\alpha = \alpha_{AT} = 1°$ and $\alpha = \alpha_{AT} = 2°$. The data point at $\alpha = \alpha_{AT} = 0$ one knows before the experiment. By judicious use of the carpet-plotting technique, all the other data points between $\alpha = \alpha_{AT} = 0$ and $\alpha = \alpha_{AT} = 2°$ were obtained. The only assumption used in obtaining these data points is that the linear $\alpha$-dependence

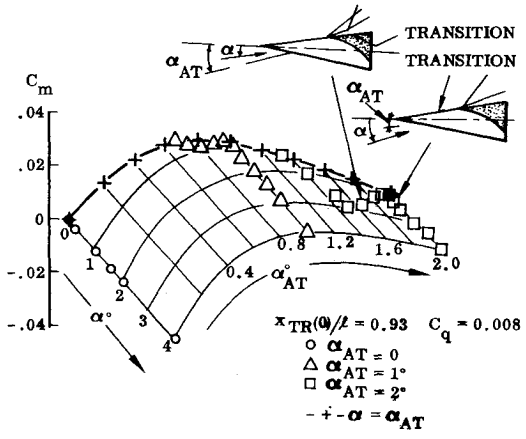


Fig. 2 Carpet plot of combined effect of $\alpha$ and $\alpha_{AT}$.

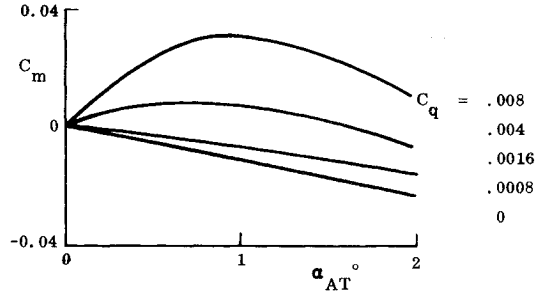


Fig. 4 Effect of asymmetric blowing rate on $C_m(\alpha_{AT})$.

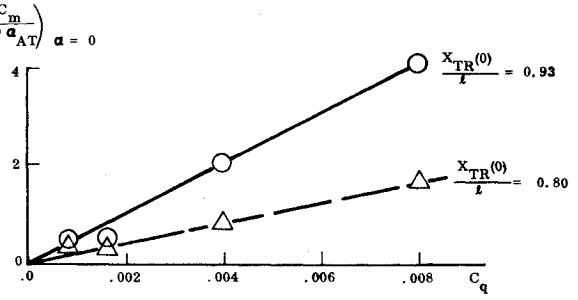


**Fig. 5 Incremental blowing-induced stability derivative at $\alpha = 0$ as a function of blowing rate.**

shown to exist in the $\alpha$-range $\alpha_{AT} < \alpha < 4°$ for $\alpha_{AT} = 0°$, 1°, and 2° also would exist for other intermediate $\alpha_{AT}$-values. It is hard to visualize any flow phenomenon that would invalidate this assumption. On the other hand, the local slopes used at $\alpha = \alpha_{AT}$ in obtaining the original fairing imply that $\partial C_m/\partial \alpha_{AT} = \partial C_m/\partial \alpha$; i.e., the transition movement derivative is assumed to be zero, $\partial x_{TR}/\partial \alpha = 0$, contrary to experimental evidence.[11]

Carpet-plotting the data[3] also for the other blowing rates gives the results shown in Fig. 4. At all blowing rates the destabilizing effect of asymmetric blowing is largest at small angles of attack near $\alpha_{AT} = 0$. One notices with some concern that the $C_m(\alpha)$-slope is negative for zero blowing rate, contrary to the measured effect of "free" asymmetric transition on a smooth solid model.[2] The reason for this anomaly is the "breathing" through the porous skin. It has been found that a porous skin model has substantially less $C_{N\alpha}$ than a solid model,[6,7] an effect that can be visualized to result from reduced streamline displacement due to in-flow through the high pressure side of the porous skin model. Here, in the case of the asymmetric porous skin configurations for $\alpha_{AT} = 1°$ and $\alpha_{AT} = 2°$, this would mean that the porous skin side is less effective in displacing the freestream and, as a consequence, a loss of leeside-to-windward-side pressure differential results. The associated gain in aft body normal force explains the statically stabilizing effect of asymmetric porous skin geometry shown in Fig. 4 for $C_q = 0$.

The incremental effects of blowing on the static stability derivative $C_{m_\alpha}$ at $\alpha = 0$, obtained from Fig. 4 for $X_{TR}(0)/ = 0.93$, are shown in Fig. 5. Also shown are the data for the other aft body asymmetric blowing configuration tested, i.e., $X_{TR}(0)/ = 0.80$. The results indicate that the destabilizing effect of asymmetric aft body blowing increases linearly with the blowing rate, and that the effect decreases in magnitude when the mean transition point, $X_{TR}(0)/l$, moves forward towards the center of gravity, $X_{CG}/l = 0.60$, all in agreement with the theoretical and experimental results shown in Ref. 2.

### References

[1] Martellucci, A. and Neff, R. S., "The Influence of Asymmetric Transition on Re-Entry Vehicle Motion," *Journal of Spacecraft and Rockets*, Vol. 8, No. 5, May 1971, pp. 476–482.

[2] Ericsson, L. E., "Transition Effects on Slender Vehicle Stability and Trim Characteristics," *Journal of Spacecraft and Rockets*, Vol. 11, No. 1, Jan. 1974, pp. 3–10.

[3] Martellucci, A., "Asymmetric Transition Effects on the Static Stability and Motion History of a Slender Vehicle," SAMSO TR-70-141, 1970, Space and Missiles Systems Organization, Los Angeles Air Force Base, Calif.

[4] Reding, J. P. and Ericsson, L. E., "Dynamic Support Interference," *Journal of Spacecraft and Rockets*, Vol. 9, No. 7, July 1972, pp. 547–553.

[5] Eckstrom, D. J., "The Influence of Mass and Momentum Transfer on the Static Stability and Drag of a Slender Cone—An Experimental Correlation," LMSC/D051269, July 1968, Lockheed Missiles & Space Co., Sunnyvale, Calif.

[6] Wimberly, C. R., McGinnis, F. K., III, and Bertin, J. J., "Transpiration and Film Cooling Effects for a Slender Cone in Hypersonic Flow," *AIAA Journal*, Vol. 8, No. 6, June 1970, pp. 1032–1038.

[7] Ericsson, L. E. and Guenther, R. A., "Dynamic Instability Caused by Forebody Blowing," *AIAA Journal*, Vol. 11, No. 2, Feb. 1973, pp. 231–233.

[8] Bertin, J. J., McCloskey, M. H., Stalmach, C. J., and Wright, R. L., "Effect of Mass-Addition Distribution and Injectant on Heat Transfer and Transition Criteria," AIAA Paper 72-183, San Diego, Calif., 1972.

[9] Jecmen, D. M., Reding, J. P., and Ericsson, L. E., "An Application of Automatic Carpet Plotting to Wind-Tunnel Data Reduction," *Journal of Spacecraft and Rockets*, Vol. 4, No. 3, March 1967, pp. 408–410.

[10] Jecmen, D. M., "Automatic Carpet Plotting," LMSC 80563, Jan. 1967, Lockheed Missiles & Space Co., Sunnyvale, Calif.

[11] Ericsson, L. E., "Correlation of Attitude Effects on Slender Vehicle Transition," *AIAA Journal*, Vol. 12, No. 4, April 1974.

# Cylindrical Wing-Body Configurations for Space-Limited Applications

D. E. SWANSON* AND C. T. CROWE†
*Washington State University, Pullman, Wash.*

### Nomenclature

$a_{-1}$ = residue
$b$ = wing span
$C_L$ = coefficient of lift
$L$ = lift force
$r$ = body radius
$S$ = cross-sectional area
$U_\infty$ = freestream velocity
$V_n$ = normal component of velocity
$w$ = complex potential
$x, y$ = abscissa and ordinate in crossflow plane, respectively
$Y$ = side force
$z$ = streamwise coordinate
$Z$ = complex variable in crossflow plane
$Z_w$ = location of the wing in the $Z_3$-plane
$\alpha$ = angle of attack
$\gamma$ = vortex strength distribution
$\zeta$ = distance along vortex sheet
$\Lambda$ = aspect ratio
$\xi$ = complex function for the body axis
$\rho$ = freestream density

*Subscripts*

1, 2, 3 = first, second, and third complex planes
$B$ = base plane of vehicle
$\infty$ = freestream

### Introduction

THE design of a vehicle with cruise capability which can be stored in a limited space usually involves the use of lifting surfaces which can be hinged or folded to satisfy the volume constraint. Several concepts for hinged and foldable wings are well-known. One such concept is the "scissor wing" which is hinged about its leading edge and swings out from a cavity in the fuselage. The primary disadvantage of this design is the reduction in load-carrying capacity and over-all utility of the vehicle due to the cavity in the fuselage. Another concept is the parawing, which is a flexible wing suspended by lines from

Received June 25, 1973; revision received September 10, 1973.
Index category: LV/M Aerodynamics.

* Graduate Student, Master's degree, Department of Mechanical Engineering.
† Associate Professor, Department of Mechanical Engineering. Member AIAA.